



Influence of the Zn plasma kinetics on the structural and optical properties of ZnO thin films grown by PLD

J. A. Guerrero de León¹ · A. Pérez-Centeno² · G. Gómez-Rosas² · A. Mariscal³ · R. Serna³ · M. A. Santana-Aranda² · J. G. Quiñones-Galván²

© Springer Nature Switzerland AG 2019

Abstract

We analyze the effect of the average kinetic energy of Zn ions on the crystalline orientation and quality, along with its effect on the optical response of ZnO thin films deposited by reactive pulsed laser deposition. With the use of laser attenuators, the Zn plasma density was kept constant while the mean kinetic ion energy was varied from 40 to 100 eV. The results show that the films are polycrystalline with a preferential orientation along the [101] direction. As the mean kinetic energy of the ions in the plasma is increased, the degree of crystallinity decreased. The preferred orientation was found to be a plasma-related effect. As deposited films show high transmittance in the visible range and an intense UV photoluminescence emission, which is associated to the excitonic recombination.

Keywords ZnO thin films · Pulsed laser deposition · Time-of-flight · Plasma kinetics

1 Introduction

Semiconductor oxides offer interesting advantages for a large range of applications (transparent electronics, transistors, sensors, memristors, electrochromic devices, photovoltaics, displays, etc.), along with low manufacturing costs [1, 2]. In particular, zinc oxide (ZnO) is a promising semiconductor for optoelectronic applications because it has a direct band gap (E_g) of 3.37 eV at room temperature (RT), it is transparent in the visible range (400–700 nm), and it has an excitonic binding energy of 60 meV [3, 4]. It can offer light emissions in the visible range, which are attributed to intrinsic defects such as zinc interstitials (Zn_i), zinc vacancies (V_{Zn}), oxygen vacancies (V_O), oxygen interstitials (O_i) and oxygen antisites (O_{Zn}) [5–7]. Additionally, ZnO presents nonlinear optical properties that can be used in applications such as frequency converters and

logic elements in the nanoscale optoelectronic circuitry [8, 9].

When grown as a thin film [5], in which thickness variation (size effect), substrate type and annealing have an effect on the optical properties [10], it can be used to fabricate UV light-emitting diodes and transparent thin-film transistors. The properties of ZnO thin films have been widely studied for a large variety of deposition methods and experimental conditions. These methods include chemical vapor deposition (CVD) [11], sol-gel [12], RF magnetron sputtering [13, 14] and pulsed laser deposition (PLD) [7, 15, 16].

PLD has proven to be an efficient method to generate thin films given that high kinetic energies of the laser-produced plasmas can be produced [17]. These energy conditions, along with directionality in the plasma, give to PLD advantages for deposition using background reactive gasses, since the reactions required to achieve the

✉ J. G. Quiñones-Galván, jose.quinones@academicos.udg.mx | ¹Departamento de Ingeniería de Proyectos, CUCEI Universidad de Guadalajara, Blvd. Marcelino García Barragán, 44430 Guadalajara, Jal., Mexico. ²Departamento de Física, CUCEI Universidad de Guadalajara, Blvd. Marcelino García Barragán, 44430 Guadalajara, Jal., Mexico. ³Laser Processing Group, Instituto de Óptica “Daza de Valdés”, IO, CSIC, Serrano 121, 28006 Madrid, Spain.



desired oxide stoichiometry are more effective [17]. The physical properties of ZnO thin films grown by PLD have been widely studied, regarding the influence of substrate [18–21] and annealing temperature [5, 6, 22], oxygen pressure [6, 7, 15, 23], substrate type (quartz [24], silicon [25], diamond-like carbon [26], sapphire [9] or glass [27]) and targets [28]. Furthermore, experimental parameters, as well as the deposition techniques, have been optimized to achieve materials with high crystalline quality [29, 30].

To the authors' knowledge, there are no studies concerning the influence of plasma parameters on the crystalline quality and optical properties of pulsed laser deposited ZnO thin films. In the present work, the synthesis of ZnO thin films at room substrate temperature, at low working pressure and using a metallic Zn target is studied. The growth of ZnO thin films at room temperature provides important advantages for the use of polymeric substrates, which is of special interest for applications on flexible electronics, e.g., the fabrication of flexible thin-film transistor (TFT) or as transparent conductive oxides (TCOs) for flexible devices [31, 32].

The possibility to achieve high crystalline quality in the grown ZnO thin film by controlling the laser energy density incident on the target surface is explored. Furthermore, a study of the laser-induced plasma kinetics by Langmuir planar probe measurements [16, 33, 34] correlated with the crystalline quality and optical response of the films is applied. Careful control of Zn ion mean kinetic energy (E_k), enables a good control of the physical properties of the deposited films. This might seem trivial; however, this control is essential when the crystalline films are produced at room temperature with no need for post-deposition annealing, as usually reported in most of the works up to the date. In addition, it is shown that the modification of the kinetic energy leads to the growth in an unexpected crystalline orientation. This could affect the properties of ZnO thin films, for instance, the stability of p-type conduction [35]. Hence, it is interesting to study the changes in crystalline orientation because this will widen the possibility of integration with different semiconductors.

2 Materials and methods

The fundamental emission line of a Nd:YAG laser (1064 nm), with a 10 Hz repetition rate and a pulse width of 6 ns, was used for the ablation of a high-purity Zn target (99.99%, from Plasmaterials), rotating at 15 rpm in order to avoid drilling. The chamber was evacuated to a base pressure of 5×10^{-5} Torr, and during the deposition, a working pressure of 2×10^{-2} Torr was set, using a background gas mixture of O₂/Ar (20/80) as reactive atmosphere. The ZnO thin films were deposited on Si (100) and

glass substrates at RT. The target to substrate distance was 5 cm. Deposition time was 30 min for all the samples. Zn ions were detected using a Langmuir planar probe [33, 36] connected to a negative potential (−48 V) and coupled to an oscilloscope in order to measure the voltage drop across a 20-Ω resistor. The oscilloscope was triggered using a photodetector that collects laser reflections. TOF signals were obtained from the oscilloscope to calculate the mean kinetic energy (E_k) of the plasma, using the following relationship [37]:

$$\langle E_k \rangle = \frac{md^2}{2} \frac{\int_0^T t^{-2} I(t) dt}{\int_0^T I(t) dt}, \quad (1)$$

where m is the ionic mass, d is the distance between target and substrate, I is the ion probe current intensity and t is the time. The maximum value of the ion probe current represents the saturation current; this is used to calculate the plasma density (N_p) following the procedure described by Doggett [33]:

$$N_p = \frac{I_{\max}}{evA}, \quad (2)$$

where e is the electron charge, v is the plasma flow velocity and A is the collecting area of the probe. In order to have different mean kinetic energies of the Zn ions (E_k) and constant plasma density ($N_p = 1 \times 10^{13} \text{ cm}^{-3}$), the incident laser energy along with the focusing spot size on the target was varied.

The crystallinity of the samples was determined by XRD with a Panalytical Empyrean diffractometer system. The optical absorption of the films was measured by UV–Vis spectroscopy with a Thermo Genesys spectrophotometer. Photoluminescence (PL) spectroscopy measurements were carried out using a 355-nm solid-state laser for excitation, and the emission was collected using a monochromator coupled with a photomultiplier tube (EMI 9659QB Extend), through lock-in technique. The film thicknesses were obtained by ellipsometric analysis using a VWASE Woollam spectroscopic ellipsometer, in the 300–1800 nm spectral range.

3 Results

Time-of-flight curves for the whole set of experiments are plotted in Fig. 1, with E_k variations from 40 to 100 eV, in 20 eV increments. As it can be seen in the TOF curves, the signal heights are almost the same for every curve, meaning that a constant value of maximum current was obtained, i.e., constant plasma density. On the other hand, the shift to shorter times represents faster reaching of the

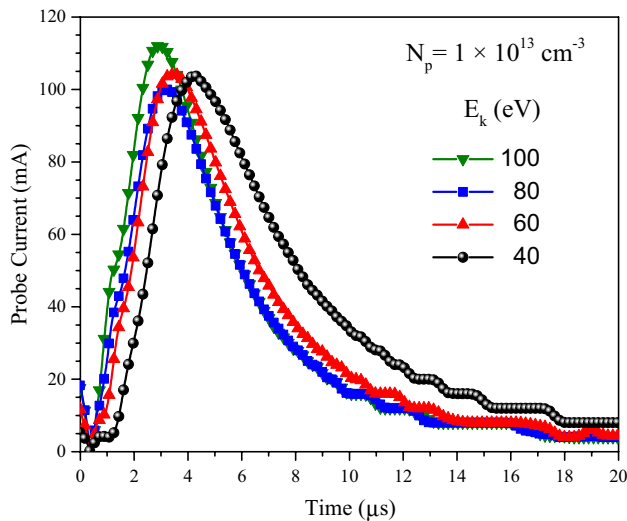


Fig. 1 TOF signals corresponding to different mean kinetic energies of the plasma

Langmuir probe, as a result of increasing kinetic energy (higher speeds).

The XRD patterns of ZnO thin films deposited on Si substrates are shown in Fig. 2a. Intensities of the

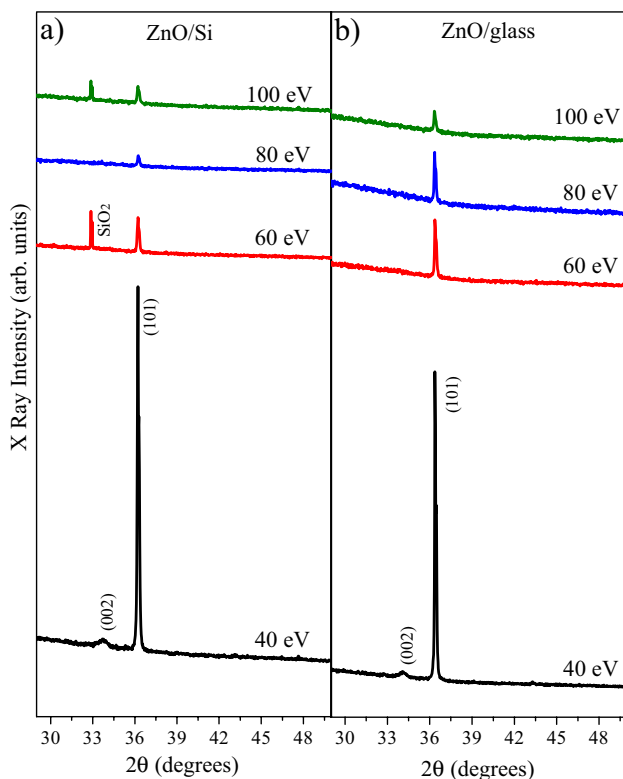


Fig. 2 XRD patterns for ZnO thin films grown at 40, 60, 80 and 100-eV mean kinetic energies of the plasma on **a** Si substrate and **b** glass substrate

crystalline profile were divided by its respective thickness obtained by ellipsometry, in order to disregard intensity variations as an effect of sample volume. A signal related to SiO₂ can be observed in all the patterns, and it is attributed to oxidation of the Si substrate. The XRD pattern of the film deposited with a mean kinetic energy of 40 eV reveals the presence of a strong diffraction peak at 36.2° and a weak peak at 33.6°, corresponding to the (101) and the (002) planes of Wurtzite phase ZnO, respectively (PDF card #36-1451). Figure 2b shows the XRD patterns corresponding to the ZnO thin films grown on glass substrates using the same experimental conditions.

Thickness and crystallite size values for the different samples are shown in Table 1. The average crystallite sizes were calculated with Scherrer equation [15]:

$$D = \frac{0.9\lambda}{\beta \cos\theta'} \tag{3}$$

where λ , θ and β are the X-ray wavelength, the Bragg angle and the FWHM of the (101) diffraction peak, respectively. Crystallite sizes were between 75 and 88 nm for samples grown within the range 60–100 eV, while for the sample grown at 40 eV, it was 107 nm.

The UV–Vis transmittance spectra of the samples deposited on glass substrates are shown in Fig. 3a. Absorption band edge is found around 375 nm for the entire set of samples. The average transmittance for the film grown at 40 eV is 80%; meanwhile, films grown at 60, 80 and 100 eV show higher average transmittances, around 85%.

Figure 3b shows the $(O.D. \times E)^2$ versus E plots, where O.D. stands for the optical density and E is the photon energy. The band gap (E_g) of the films was estimated by extrapolating the linear part of the plot to the E axis as shown in Fig. 3b.

PL spectra normalized with respect to films thicknesses are shown in Fig. 4. An intense UV emission around 377 nm (~3.3 eV) can be observed for all samples, related to excitonic recombination. The inset of Fig. 4 shows the peak position as a function of the plasma energy.

Table 1 Mean kinetic energy, thickness, crystallite size, band gap (E_g) of ZnO/Si thin films and FWHM values from XRD patterns

Mean kinetic energy (eV)	Thickness (nm)	Crystallite size (nm)	Band gap (eV)	FWHM of XRD (°)
100	60	84	3.21	0.11
80	46	88	3.17	0.10
60	44	75	3.21	0.11
40	66	107	3.35	0.08

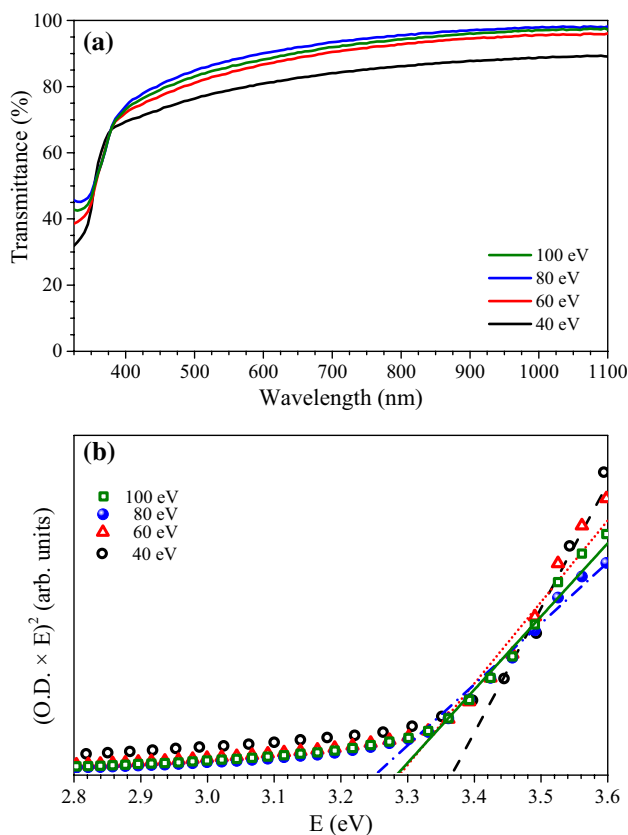


Fig. 3 **a** Optical transmittance and **b** band gap estimation of ZnO thin films

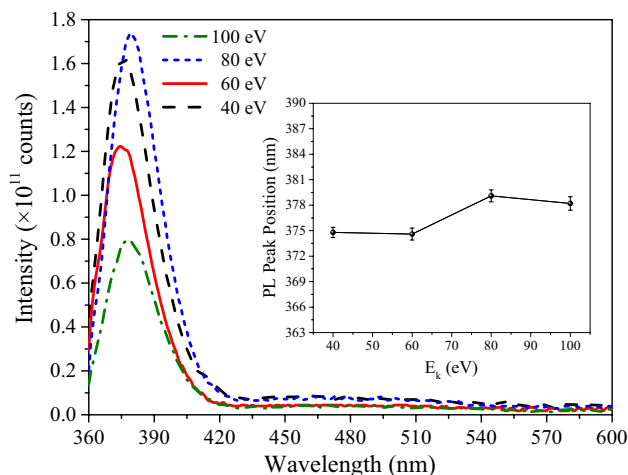


Fig. 4 PL spectra normalized with thickness of ZnO thin films deposited with different mean kinetic energies of the plasma. The inset shows the peak position as a function of the plasma energy

4 Discussion

In the XRD patterns (Fig. 2) when the ion mean kinetic energy increases to 60 eV, the (101) peak losses intensity and the (002) peak is not observed anymore. At 80 eV, the (101) peak can still be observed, but with a weaker intensity. There is not a significant change at 100 eV in the XRD pattern. The polar nature of ZnO is widely known, and there are many reports showing films strongly oriented in the [002] direction [18–22, 24, 26, 35, 38]. However, according to these results, our PLD synthesis conditions favor the crystal growth in the [101] direction that barely has been reported before [6, 15, 39]. These XRD patterns show the same preferred orientation along the [101] direction. Figure 2b (ZnO thin films grown on glass) confirms that preferred growth orientation is an effect of plasma conditions and it does not depend on the substrate material; neither its crystallinity nor its surface orientation. The preferred orientation in the [101] direction is presumably induced by internal stress, caused by the surface mobility of the species arriving to the substrate at RT [39]. On the other hand, high working pressure in oxygen-containing reactive atmosphere ($> 10^{-1}$ Torr) can be favorable for the formation of the intense (101) peak when using PLD [6, 15, 39]. However, in our case, control of E_k (at 2×10^{-2} Torr) leads to similar results to those using high working pressures. It has been discussed in the literature that in laser produced plasmas, out-of-equilibrium processes are expected to exist, leading to the growth of metastable phases or uncommon preferred orientations [37, 40].

The increase in the intensity of XRD signals is always accompanied by the decrease in the full width at half maximum (FWHM); such issue supports the increasing and the enhancement of materials crystallization or the order of the material. The obtained data confirm that the crystalline order of our material through the orientation (101) is bigger than the order on the orientation (002); this implies that the crystallite size through the orientation (101) is larger than through the orientation (002). Also, it has been reported that the energy fluence has strong effects in the crystallinity of ZnO thin films [41], and in particular, high fluence levels readily cause the degradation of film quality owing to the incorporation of high-energy species [42]. In this work, we obtained the best thin film crystallinity at low-energy fluence (leading to $E_k = 40$ eV), which is in agreement with previous works. Besides, in pulsed laser deposition, the energy difference between the Zn ions impinging the substrate at low E_k (40 eV) and the surface energy of the substrate causes a reduction in the surface mobility, promoting the growth in an atypical direction [43]. For the case of

samples grown at the range of 60–100 eV, less efficient crystallization processes (increased amorphicity) can be attributed to the increase in surface mobility that allows species to reach low-energy sites at the substrate.

The difference in grain sizes (see Table 1) is related to the surface mobility, which allows the high-energy species of samples grown at 60–100 eV to move and coalesce in smaller grains than sample grown at 40 eV, in which species do not have enough mobility to reach lower surface energy sites. These results are in agreement with results regarding crystallization of the films. Therefore, in samples grown at 60–100 eV, high mobility is compensated with longer reaction time, leading to no significant changes in its crystallization process. The FWHM values shown in Table 1 are lower compared with literature reports [7, 19, 26], indicating that the samples exhibit high structural quality.

The UV–Vis transmittance spectra result (Fig. 3a) show that there is a slight increasing trend in transmittance along with the plasma energy. However, sample grown at 100 eV showed a small decrease, compared with sample grown at 80 eV; this effect is most likely related to the higher thickness of the film deposited at 100 eV (see Table 1).

The E_g values shown in Table 1 are similar to those reported in literature [5–7]. Note that the highest E_g value corresponds to the film grown at 40 eV, which according to XRD results has a higher crystalline quality, this band gap value is near to the reported value of high-quality ZnO [3, 4]. As the plasma energy increased, the optical band gap values decreased. This behavior can be explained by the loss of crystalline quality of the samples, as revealed by XRD results. Intrinsic defects lead to stress in the material, which results in a less homogeneous lattice that can induce a reduction in crystallinity; at the same time, the intrinsic defects introduce localized states that modify E_g values. In samples grown at energies between 60 and 100 eV, it is probable that an oxygen deficiency allowed the introduction of localized defect states, possibly related to Zn excesses like Zn_i , which causes a band gap narrowing [18].

In PL spectra (Fig. 4), a slight shift to larger wavelengths (lower energies) is observed as the kinetic energy increases. This result is in agreement with the band gap values obtained from UV–Vis measurements and the loss of crystallinity observed by XRD analysis. A weak blue emission from deep level is observed around 480 nm (2.7–2.5 eV). This is associated with the transition from zinc interstitials (Zn_i) to zinc vacancies (V_{Zn}) [5–7, 11–13, 15]. In contrast, the common green emission around 530 nm, (~ 2.5 – 2.2 eV), associated to transitions from conduction band to oxygen antisites vacancies (O_{Zn}) or oxygen interstitials (O_i) [25], has not been

observed in these samples. The relative low emission in the visible region ($I_{480}/I_{377} \sim 0.05$) for all samples is an indicator of the low density of intrinsic defects in the films, as well as stoichiometric growth of ZnO. This characteristic is desirable for the fabrication of optical components and transistors since it avoids losses due to the defects, increasing the excitonic recombination, which is intrinsically related to the semiconductor behavior of the material. The high intensity of the UV band together with the absence or low intensity of defect-associated bands is an indicative of the excellent crystalline quality of the films, confirming the results obtained from XRD. It is worth mentioning that even though a reduction in crystallinity was observed for increasing plasma energy, the optical quality of the films was not significantly affected.

5 Conclusions

Preferential (101) orientation in pulsed laser-deposited ZnO thin films has been achieved by the laser ablation of metallic Zn in an oxygen-containing atmosphere. It was observed that this uncommon growth is an effect of the plasma mean kinetic energy. A decrease in crystallinity was observed when energy increased from 40 to 60 eV; however, no significant changes were observed between samples grown with 60 eV and over, since the high mobility of Zn ions is compensated with longer reaction time. Thin films have high average transmittances between 80 and 85% and optical band gap between 3.35 and 3.17 eV. PL spectra of all samples showed an intense emission around 377 nm (UV) and a weak blue emission around 480 nm. The first signal is associated with the excitonic recombination and is indicative of the good crystalline quality of the films. The 480-nm signal is a deep level emission, indicative of intrinsic defects; zinc interstitials (Zn_i) and zinc vacancies (V_{Zn}). The decrease in the first with the increase in E_k is therefore related to the reduction in the crystalline quality of the films due to the appearance of defects, such as zinc interstitials (Zn_i) and zinc vacancies (V_{Zn}).

According to the present results, the control of the mean kinetic energies of the plasma in PLD is an excellent method to produce ZnO thin films with good optical quality, uncommon crystalline orientation and low density of intrinsic defects.

Acknowledgements Authors want to thank the technical assistance of Sergio Oliva (U de G), as well as the financial support from CONACYT (Grant: CB2010-156773), Universidad de Guadalajara (pro-SNI). JAGdeL wants to thank CONACYT for a PhD scholarship, as well as the financial support from Doctorado en Ciencia de Materiales, CUCEI, U de G (program PROINPEP).

Author's contribution All authors contributed to complete the manuscript in the data analyses and prepared the manuscript. J.A.G.L, J.G.Q.G. and M.A.S.A. performed the experimental design and carried out the deposition of the samples. A.P.C. and G.G.R. contributed to the analysis of UV–Vis and XRD. A.M. and R.S. performed the ellipsometry and PL characterizations and analyses of the samples.

Compliance with ethical standards

Conflict of interest The authors declare that they have no conflict of interest.

References

- Wang Z, Nayak PK, Caraveo-Frescas JA, Alshareef HN (2016) Recent developments in p-type oxide semiconductor materials and devices. *Adv Mater* 28:3831–3892. <https://doi.org/10.1002/adma.201503080>
- Fortunato E, Barquinha P, Martins R (2012) Oxide semiconductor thin-film transistors: a review of recent advances. *Adv Mater* 24:2945–2986. <https://doi.org/10.1002/adma.201103228>
- Kumar ES, Singh S, Rao R (2014) Zinc oxide: the versatile material with an assortment of physical properties. In: Ramachandra Rao MS, Okada T (eds) *ZnO nanocrystals and allied materials*, 1st edn. Springer India, New Delhi
- Zawadzka A, Płóciennik P, Strzelecki J, Sahraoui B (2014) Transparent amorphous zinc oxide thin films for NLO applications. *Opt Mater* 37:327–337. <https://doi.org/10.1016/j.optmat.2014.06.021>
- Al-Assiri MS, Mostafa MM, Ali MA, El-Desoky MM (2015) Optical properties of annealed ZnO thin films fabricated by pulsed laser deposition. *Silicon* 7:393–400. <https://doi.org/10.1007/s12633-015-9301-z>
- Ismail RA, Rasheed BG, Salm ET, Al-Hadethy M (2007) Transparent and conducting ZnO films prepared by reactive pulsed laser deposition. *J Mater Sci Mater Electron* 18:397–400. <https://doi.org/10.1007/s10854-006-9046-y>
- Zhao L, Xu C, Liu Y, Liu Y (2010) Effects of temperature and pressure on the structural and optical properties of ZnO films grown by pulsed laser deposition. *Sci China Technol Sci* 53:317–321. <https://doi.org/10.1007/s11431-010-0047-y>
- Kulyk B, Sahraoui B, Krupka O et al (2009) Linear and nonlinear optical properties of ZnO/PMMA nanocomposite films. *J Appl Phys* 106:093102. <https://doi.org/10.1063/1.3253745>
- Kulyk B, Essaidi Z, Luc J et al (2007) Second and third order nonlinear optical properties of microrod ZnO films deposited on sapphire substrates by thermal oxidation of metallic zinc. *J Appl Phys* 102:113113. <https://doi.org/10.1063/1.2822461>
- Kapustianyk V, Turko B, Kostruba A et al (2007) Influence of size effect and sputtering conditions on the crystallinity and optical properties of ZnO thin films. *Opt Commun* 269:346–350. <https://doi.org/10.1016/j.optcom.2006.08.034>
- Pedersen JD, Esposito HJ, Teh KS (2011) Direct synthesis and characterization of optically transparent conformal zinc oxide nanocrystalline thin films by rapid thermal plasma CVD. *Nanoscale Res Lett* 6:568. <https://doi.org/10.1186/1556-276X-6-568>
- Fuertes V, Mariscal A, Serna R et al (2017) Multifunctional ZnO/Fe–O and graphene oxide nanocomposites: enhancement of optical and magnetic properties. *J Eur Ceram Soc* 37:3747–3758. <https://doi.org/10.1016/j.jeurceramsoc.2017.02.026>
- Dang WL, Fu YQ, Luo JK et al (2007) Deposition and characterization of sputtered ZnO films. *Superlattices Microstruct* 42:89–93. <https://doi.org/10.1016/j.spmi.2007.04.081>
- Kulyk B, Sahraoui B, Figà V et al (2009) Influence of Ag, Cu dopants on the second and third harmonic response of ZnO films. *J Alloys Compd* 481:819–825. <https://doi.org/10.1016/j.jallcom.2009.03.117>
- Fan XM, Lian JS, Jiang Q, Zhou Z (2007) Effect of the oxygen pressure on the photoluminescence properties of ZnO thin films by PLD. *J Mater Sci* 42:2678–2683. <https://doi.org/10.1007/s10853-006-1367-y>
- Strikovski MD, Kim J, Kolagani SH (2010) Plasma energetics in pulsed laser and pulsed electron deposition. In: Dhanaraj G, Byrappa K, Prasad V, Dudley M (eds) *Springer handbook of crystal growth*. Springer, Berlin, pp 1193–1211
- Chrisey DB, Hubler GK (1994) *Pulse laser deposition of thin films*. Wiley, New York
- Srinivasarao K, Rajinikanth B, Pandurangarao K, Mukhopadhyay PK (2012) Physical investigations on pulsed laser deposited nanocrystalline ZnO thin films. *Appl Phys A* 108:247–254. <https://doi.org/10.1007/s00339-012-6895-5>
- Kang SJ, Joung YH, Shin HH, Yoon YS (2007) Effect of substrate temperature on structural, optical and electrical properties of ZnO thin films deposited by pulsed laser deposition. *J Mater Sci Mater Electron* 19:1073–1078. <https://doi.org/10.1007/s10854-007-9469-0>
- Cui JB, Soo YC, Kandel H et al (2009) Investigations of ZnO thin films deposited by a reactive pulsed laser ablation. *Sci China Ser E Technol Sci* 52:99–103. <https://doi.org/10.1007/s11431-008-0339-7>
- Zhou P, Liu H, Zhang L et al (2016) Study of substrate temperature and copper doping effects on structural, electrical and optical properties of Cu-doped and undoped ZnO thin films. *J Mater Sci Mater Electron* 27:7822–7828. <https://doi.org/10.1007/s10854-016-4771-3>
- El-Desoky MM, Ali MA, Afifi G, Imam H (2014) Annealing effects on the structural and optical properties of growth ZnO thin films fabricated by pulsed laser deposition (PLD). *J Mater Sci Mater Electron* 25:5071–5077. <https://doi.org/10.1007/s10854-014-2273-8>
- Ramachandra Rao MS, Okada T (2014) ZnO nanocrystals and allied materials. In: Hull R, Jagadish C, Kawazoe Y, Parisi J, Pohl UW, Seong T-Y, Uchida S, Wang ZM, Kruzic J (eds) *Springer series in materials science*, 1st edn. Springer, New Delhi
- Uehara T, Kurumi S, Takase K, Suzuki K (2010) Synthesis of p-type zinc oxide films by plasma-assisted pulsed laser deposition. *Appl Phys A Mater Sci Process* 101:723–725. <https://doi.org/10.1007/s00339-010-5929-0>
- Lin B, Fu Z, Jia Y (2001) Green luminescent center in undoped zinc oxide films deposited on silicon substrates. *Appl Phys Lett* 79:943–945. <https://doi.org/10.1063/1.1394173>
- Li S, Zhang L, Dong Y, Zhao F (2012) Optical properties of ZnO thin films grown on diamond-like carbon by pulsed laser deposition. *Optoelectron Lett* 8:445–448. <https://doi.org/10.1007/s11801-012-2295-5>
- Bulgakov AV, Evtushenko AB, Shukhov YG et al (2010) Cluster generation under pulsed laser ablation of zinc oxide. *Appl Phys A Mater Sci Process* 101:685–689. <https://doi.org/10.1007/s00339-010-5973-9>
- Haško D, Bruncko J, Vincze A, Uherek F (2009) Comparative study of ZnO layers prepared by PLD from different targets at various oxygen pressure levels. *Cent Eur J Phys* 7:345–349. <https://doi.org/10.2478/s11534-009-0047-3>
- Opel M, Geprägs S, Althammer M et al (2014) Laser molecular beam epitaxy of ZnO thin films and heterostructures. *J*

- Phys D Appl Phys 47:034002. <https://doi.org/10.1088/0022-3727/47/3/034002>
30. Tsukazaki A, Ohtomo A, Kawasaki M (2014) Surface and interface engineering of ZnO based heterostructures fabricated by pulsed-laser deposition. *J Phys D Appl Phys* 47:034003. <https://doi.org/10.1088/0022-3727/47/3/034003>
 31. Huang JJ, Wang YP, Lu JG et al (2011) Transparent conductive Al-doped ZnO/Cu bilayer films grown on polymer substrates at room temperature. *Chin Phys Lett* 28:127306. <https://doi.org/10.1088/0256-307X/28/12/127306>
 32. Gupta M, Chowdhury FR, Barlage D, Tsui YY (2013) Optimization of Pulsed Laser Deposited ZnO thin-film growth parameters for thin-film transistors (TFT) application. *Appl Phys A Mater Sci Process* 110:793–798. <https://doi.org/10.1007/s00339-012-7154-5>
 33. Doggett B, Lunney JG (2009) Langmuir probe characterization of laser ablation plasmas. *J Appl Phys* 105:33306. <https://doi.org/10.1063/1.3056131>
 34. Williams GO, O'Connor GM, Mannion PT, Glynn TJ (2008) Langmuir probe investigation of surface contamination effects on metals during femtosecond laser ablation. *Appl Surf Sci* 254:5921–5926. <https://doi.org/10.1016/j.apsusc.2008.03.192>
 35. Dai L, Wang S, Zhong Z, Zhang G (2014) Properties of p-type ZnO thin films with different orientations. *Optoelectron Lett* 10:111–114. <https://doi.org/10.1007/s11801-014-3230-8>
 36. Franz G (2009) *Plasma Diagnostics. Low pressure plasmas and microstructuring technology*. Springer, Berlin, pp 1–732
 37. Quiñones-Galván JG, Camps E, Campos-González E et al (2015) Influence of plasma parameters and substrate temperature on the structural and optical properties of CdTe thin films deposited on glass by laser ablation. *J Appl Phys* 118:125304. <https://doi.org/10.1063/1.4931677>
 38. Fabbri F, Villani M, Catellani A et al (2014) Zn vacancy induced green luminescence on non-polar surfaces in ZnO nanostructures. *Sci Rep* 4:5158. <https://doi.org/10.1038/srep05158>
 39. Angappane S, Selvi NR, Kulkarni GU (2009) ZnO(101) films by pulsed reactive crossed-beam laser ablation. *Bull Mater Sci* 32:253–258. <https://doi.org/10.1007/s12034-009-0038-4>
 40. Quiñones-Galván JG, Lozada-Morales R, Jiménez-Sandoval S et al (2016) Physical properties of a non-transparent cadmium oxide thick film deposited at low fluence by pulsed laser deposition. *Mater Res Bull* 76:376–383. <https://doi.org/10.1016/j.materresbull.2016.01.002>
 41. Craciun V, Elders J, Gardeniers JGE, Boyd IW (1994) Characteristics of high quality ZnO thin films deposited by pulsed laser deposition. *Appl Phys Lett* 65:2963–2965. <https://doi.org/10.1063/1.112478>
 42. Zeng JN, Low JK, Ren ZM et al (2002) Effect of deposition conditions on optical and electrical properties of ZnO films prepared by pulsed laser deposition. *Appl Surf Sci* 198:362–367
 43. Gorbunoff A (2007) Cross-beam PLD: metastable film structures from intersecting plumes. In: Eason R (ed) *Pulsed laser deposition of thin films: applications-led growth of functional materials*. Wiley, Hoboken, pp 131–155

Publisher's Note Springer Nature remains neutral with regard to jurisdictional claims in published maps and institutional affiliations.